

# Dynamic Simulation and Exergy Analysis of an Organic Rankine Cycle Integrated with Vapor Compression Refrigeration System

Prateek D. Malwe<sup>a,b,\*</sup>, Juned Shaikh<sup>a</sup>, Bajirao S. Gawali<sup>a</sup>, Hitesh Panchal<sup>c</sup>, Ahmet Selim Dalkilic<sup>d</sup>, R. Saidur<sup>e,f</sup>, Ali Jawad Alrubaie<sup>g</sup>

<sup>a</sup>Department of Mechanical Engineering, Walchand College of Engineering Sangli, Shivaji University, Kolhapur Maharashtra 416415, India

<sup>b</sup>Department of Mechanical Engineering, Dr. D. Y. Patil Institute of Technology, Pimpri, Pune, S.P.P.U., Maharashtra 411014, India

<sup>c</sup> Department of Mechanical Engineering, Government College of Engineering, Patan, Gujrat 384265, India

<sup>d</sup>Department of Mechanical Engineering, Yildiz Technical University, Istanbul 34349, Turkey

<sup>e</sup> Research Centre for Nano-Materials and Energy Technology (RCNMET), School of

Science and Technology, Sunway University, Bander Sunway, Petaling Jaya, 47500, Selangor, Darul Ehsan, Malaysia

<sup>f</sup>Department of Engineering, Lancaster University, Lancaster LA1 4YW, UK

<sup>g</sup>Department of Medical Instrumentation Techniques Engineering, Al-Mustaqbal University College, Babylon, Iraq

## Abstract

Organic Rankine Cycle (ORC) has consistently been demonstrated to be one of the most effective and reliable methods for extracting low-grade waste heat energy. Research works including simulations and experimentations with considerable refrigerants are carried out to investigate the performance analyses of an integrated system. The objective of this study is to analyze the integrated vapor compression refrigeration system (VCRS)-ORC system, for which a custom model is built on MATLAB-Simulink, and refrigerant properties are imported from the Coolprop database. This methodology allowed the authors to perform dynamic analysis of the system for varying VCRS evaporator temperature, VCRS load, and VCRS condenser temperature, and that too with different refrigerants considered making a total of 150 combinations. Research works use Engineering Equation Solver (EES) or MATLAB to simulate systems, which has limited capabilities in terms of dynamic analysis and the number of refrigerants selected for the analysis. This however is not the case with the methodology followed in this research work. The model developed for the dynamic simulation and performance assessment of the integrated VCRS-ORC system is verified. For dynamic simulation, the VCRS load, evaporator, and condenser temperatures are varied from 1 TR to 10 TR, 0 °C to 10 °C, and 45 °C to 60 °C, respectively. From the exergy analysis, it is found that, in comparison to all combinations, the best performance is obtained for the R141b–R1234ze(Z) pair as the ORC and VCRS refrigerant respectively. The performance parameters for this combination give a maximum system overall exergy efficiency of 33.045 %, a maximum net Coefficient of Performance of 4.593, and the least exergy destruction of 2.591 kW. The net Coefficient of Performance increases from 3.9 to 5.5 as the evaporator temperature rises, but the turbine work decreases from 84.5 W to 78.5 W. However, these parameters show an inverse trend with a rise in the condenser temperature. Based on the simulations, the integrated vapor compression refrigeration system - Organic Rankine Cycle system has a 10.62 % higher Coefficient of Performance than the refrigeration system for the R141b–R1234ze(Z) refrigerant pair.

**Keywords:** Organic Rankine Cycle; waste heat; exergy analysis; dynamic simulation; vapor compression refrigeration system; exergy efficiency

\*Corresponding author. Tel.: +91-9404582917; ORCID: <https://orcid.org/0000-0003-4576-9318>;

E-mail address: [prateek.malwe@walchandsangli.ac.in](mailto:prateek.malwe@walchandsangli.ac.in)

39 **1. Introduction**

40 The dependence of humans on the consumption of energy has increased drastically during the last few  
41 years. It causes a huge consumption of fossil fuels which creates certain environmental issues. According  
42 to the survey by Mahmoudi et al. [1], about 50 % of the world's energy is available in the form of waste  
43 heat. The various sources of heat energy like internal combustion engines, household waste, geothermal,  
44 solar radiation, steam and gas turbines, etc. are available. This waste heat can be recovered and used to  
45 produce a useful power output. Wahile et al. [2], suggested that there are many other ways to utilize this  
46 waste heat by using the phase change materials. However, the use of an ORC offers certain advantages  
47 over other waste heat recovery systems like a requirement of no land, large potential utilization factor, is  
48 of manufacture, easy availability of components, flexibility, low maintenance requirement, safe, cheaper,  
49 showing better thermal performance, etc. [3]. As organic fluids have a lower boiling point than water,  
50 this allows recovering energy from low-temperature waste heat resources. The thermal efficiency of ORC  
51 is a function of working fluid temperature, the temperature of the heat source, and the sink. In general, its  
52 value lies between 2 % to 19 %. Malwe et al. [4] conducted a comprehensive review of the usage of an  
53 ORC as a method of waste heat recovery, citing it as one of the most prominent and efficient methods.  
54 The results of an exergetic analysis of heat extraction from a VCRS using 29 distinct potential ORC fluids  
55 and an integrated VCRS-ORC system are presented. In this paper, VCRS and ORC systems are integrated  
56 to have energy conservation by tapping the waste heat. The objective of the study is to make use of the  
57 waste heat from the refrigeration system's condenser as a means of waste heat recovery to run an ORC;  
58 thereby producing a power output from the waste heat. Aside from that, further ORC characteristics such  
59 as working fluid selection, thermodynamics, and environmental impact on working fluid performance,  
60 among others, are examined.  
61

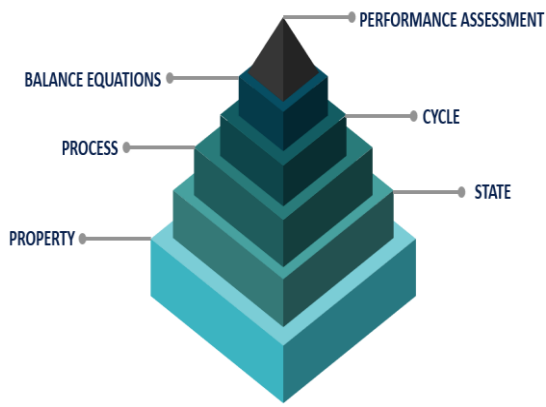


Fig. 1. A schematic representation of Dincer's six-step approach [4]



Fig. 2. A systematic representation of exergization [4]

Dincer et al. [5] emphasize the significance and necessity of doing an exergy analysis in any system. The major goal of this article is to introduce some thermodynamic dimensions to create a platform for exergization as Dincer's six-step approach is shown in Fig. 1. Exergization (Fig. 2) is the process of applying exergy analysis to improve the design and analysis of a thermal system to get an efficient system [6]. Several types of research have worked in the fields of dynamic simulation, modeling, and performance evaluation of an integrated VCRES-ORC system employing energy and exergy studies as a tool. It's further broken down into exergy analysis as a tool and ORC as a waste heat recovery method.

### *1.1. Exergy analysis as a tool*

Dincer et al. [7] have examined the role of exergy and its application by developing the AIDA concept which is relevant to all systems. Malwe et al. applied exergy analysis as a tool to evaluate the performances of thermal engineering systems like internal combustion engines [8], cryocoolers, etc. to evaluate the performances of the systems [9]. Ahamed et al. [10] examined the potential/scope of research work in the field of second analysis of a VCRES for various applications. Exergy efficiency can be improved by lowering the temperature difference between the evaporator and condenser, as well as ensuring that the refrigerant is subcooled by about 5 °C. By blending these hydrocarbons in various percentages with R134a (as a baseline), the performance of a VCRES can be improved. Compressors have the highest exergy destruction of all the components, indicating that there is room for improvement in exergy efficiency. Using nano lubricants and nanofluids instead of conventional refrigerants in the system is another way to reduce compressor exergy destruction. Anand et al. [11] conducted a refrigerant literature review that included simulated case studies. The goal of this review is to learn about the various software programs used to specify refrigeration systems. A solution heat exchanger can be used to improve the performance of an existing system. A suitable output can also be obtained by delivering solar streams at temperatures of roughly 100 °C to a vapor absorption refrigeration system. Borikar et al. [12] performed an experimental assessment on a domestic refrigerator to measure energy consumption.

Malwe et al. carried out exergy analysis [13], and management of a simple VCRES [14]. Moreover, a simulation work involving the energy and exergy assessments of a multi-stage VCRES suggesting the component-wise exergy destructions and efficiencies formulations is carried out. [15]. Jemma et al. [16] investigate the usage of R1234ze(E) as a refrigerant alternative to R134a. The results demonstrate that the compressor, condenser, expansion valve, and evaporator are in decreasing order of exergy destruction. R1234 has performance characteristics that are similar to R134a. However, as compared to R134a, the COP and exergy efficiency of R1234ze as a refrigerant is higher. R1234ze(E) has been determined to be superior to R134a in terms of performance and environmental friendliness. Babiloni et al. [17] executed the exergy analysis of a small VCRES is done using R513A as a new alternative refrigerant to R134a.

95 Compressor, evaporator, expansion valve, and condenser are in decreasing sequence of exergy  
96 destruction rate. In comparison to R-134a, Ozgur et al. [18] employed R1234yf as an alternative  
97 refrigerant in the refrigeration system, and the results reveal a lower exergy destruction value. However,  
98 one of the main issues of R1234yf is its safety. Geete et al. [19] have analyzed a VCRS using the concept  
99 of minimization of entropy and exergy destruction. The VCRS has the worst performance with a  
100 combination of 85 % R134a and 15 % R152a due to higher entropy generation and exergy destruction. As  
101 a result, a blend of 85 % R134a and 15 % R290, or R600a alone, is used as a replacement for R134a. Roy  
102 et al. [20] have thermodynamically analyzed a VCRS with R134a as a refrigerant. The modified system  
103 achieves a 3.7 % and 3.5 % increase in COP and exergy efficiency, respectively. Gaurav et al. [21]  
104 conducted the first and second analyses of a VCRS with various refrigerants such as R134a, R1234yf, and  
105 R1234ze, as well as their mixtures. Among the 31 different sets, the best performance and alternative to  
106 R134a is obtained for R134a/R1234yf (90%/10%), N13a [R134a/R1234yf/R1234ze (42%/18%/40%)],  
107 R152a and N13b [R134a/R1234ze (42%/58%)]. From an energy consumption standpoint, Shikalgar et al.  
108 [22] used a water-cooled and a hot wall air-cooled condenser alternately for a domestic refrigerator type,  
109 and different metrics such as COP, exergy efficiency, and so on are investigated. The refrigerator with the  
110 water-cooled condenser is 7 to 9 % more efficient than the refrigerator with the other type.

111 Agarwal et al. [23] used EES to investigate the energy and exergy of a simple VCRS with R1234ze  
112 and R1234yf as R134a replacements. For similar operating conditions, R1234yf performs marginally  
113 worse than R134a. R1234ze is a remarkable alternative to R134a, outperforming it by 1.8 % and 1.87 %  
114 in terms of exergy efficiency and COP, respectively when compared to R134a. Kumar et al. [24]  
115 demonstrated an exergy approach for assessing a vapor compression refrigeration system. For R11 and  
116 R12, respectively, exergy efficiencies of 49 % and 50 % were found. Fazar et al. [25] preferred R290 to  
117 replace R410a in a split air conditioning system. Instead of R410a, R290 refrigerant is used, resulting in a  
118 refrigerant need of about 45 to 55 % of the full charge of R410a, and the COP rises from 4.6 to 4.9, and  
119 compression work is reduced by 35.7 %. Arora et al. [26] investigated the performance of an actual vapor  
120 refrigeration system using R502, R404a, and R507a as refrigerants. According to the results of the  
121 investigation, R507 is a great refit to R502 when compared to R404a. R1234yf and R1234ze are labeled  
122 "*fourth-generation refrigerants*" by Yataganbaba et al. [27] since they have zero ODP and are employed  
123 as substitutes to R-134a in a two-evaporator VCRS with an evaporator pressure regulator. The results  
124 show that a multi-evaporator VCRS has a higher exergy efficiency than a single-evaporator system.  
125 Nikolaidis et al. [28] investigated a two-stage VCRS with a flash intercooler using a technology method  
126 using R22 refrigerants. By lowering the individual irreversibilities in the condenser and evaporator, the  
127 overall irreversibility rate of the plant is reduced by 2.40 and 2.78 times, respectively, compared to the  
128 original system. Anjum et al. [29] conducted a first and second law analysis of waste heat extraction from

129 the intercooler of a multi-stage VCRS utilizing ammonia refrigerant. For a  $-40\text{ }^{\circ}\text{C}$  evaporator temperature,  
130 a maximum COP of 3.087 is obtained. COP, on the other hand, decreases when the condenser  
131 temperature rises and the evaporator temperature falls. Dwinanto et al. [30] provide a step-by-step guide  
132 on designing a refrigeration system.

### 133 1.2. Waste heat recovery using ORC

134 Quoilin et al. [31], described a technological solution for ORC, a list of ORC manufacturers over the  
135 globe, etc. with a focus on the temperature levels [32]. Franchetti et al. [33] specified selection of  
136 working fluid is the basic step in ORC design. Lakew et al. [34] designed an ORC to achieve either a  
137 maximum power output or to have a smaller size of components. Six working fluids namely R123,  
138 R134a, R245fa, R227ea, R123, R134, R290, and n-pentane are considered. R227ea and R245fa produce  
139 maximum power for heat source temperatures in the range of  $80\text{ }^{\circ}\text{C} - 160\text{ }^{\circ}\text{C}$  and  $160\text{ }^{\circ}\text{C} - 200\text{ }^{\circ}\text{C}$   
140 respectively. Rajabloo [35] reveal that the performance improvement in the ORC occurs with both - pure  
141 and mixtures of working fluids due to an increase in the mass flow rate of hot source fluid. Yadav, et al.  
142 [36] explored working fluid selection from an ORC in an Indian region of  $75\text{ }^{\circ}\text{C}$  to  $80\text{ }^{\circ}\text{C}$ . R245fa  
143 outperforms all other refrigerants in terms of ORC efficiency. Tahir et al. [37] built an ORC with working  
144 fluid- R245fa having an objective function of producing lower than 1 kW of turbine power. The cold  
145 source and hot source temperatures are maintained in the temperature in the range of  $60\text{ }^{\circ}\text{C} - 100\text{ }^{\circ}\text{C}$  and  
146  $10\text{ }^{\circ}\text{C} - 30\text{ }^{\circ}\text{C}$  respectively. It is advised to make use of a largely efficient pump to have positive heat  
147 recovery. Caceres et al. [38] did the optimization of the organic Rankine cycle to select the most suitable  
148 organic fluid out of 39 different combinations of working fluids. Dai et al. [39] explored the outcome of  
149 performing parameters on ORC using 10 different organic fluids. The sizing of the turbine varies directly  
150 to the inlet-specific volume. Kaushik et al. [40] introduced a Canopus heat exchanger across the  
151 compressor and condenser with R134a and R507a as working fluids to enhance the system's COP. Sarkar  
152 et al. [41] have demonstrated a pinch point method for the analysis of an ORC for maximum heat  
153 recovery. Bonk et al. [42] presented a paper on designing a micro-ORC system of 1 kW power output. Ali  
154 [43] did effective thermal management of the electronic devices using Nickel foam along with paraffin  
155 wax by increasing the surface area of heat flow. Additionally, Shahsavar et al. [44] have investigated the  
156 laminar forced convection problem and improved with the use of holes.

157 From an efficiency point of view, Novec 649 is considered a novel organic fluid with a GWP of  
158 1.1, which is comparatively lower than R245fa. Scagnolatto et al. [45] simulated a small-scale ORC (10  
159 kW) for which R123 gives the highest exergy efficiency among the other selected refrigerants due to the  
160 presence of a recuperator. Saha [46] assured a waste heat utilization which becomes the need of an hour  
161 from environmental and energy conservation concerns. An ORC with a capacity of 20 kW was

162 numerically examined by Kong et al. [47] utilizing R 245fa as the refrigerant in the combined saturated  
163 steam/hot water resource and has the highest exergy efficiency. The exergy efficiency varies in direct  
164 proportion to the temperature of the heat source. Ozdemir [48] suggested that the power output of the  
165 regenerative ORC is higher than that of the simple/basic ORC. The thermal energy efficiency and exergy  
166 efficiency of regenerative ORC are 23.1 % and 69.9 % higher than those of simple ORC, respectively. An  
167 exergy analysis of an ORC using a geothermal heat source at 125 °C with four refrigerants was performed  
168 by Bademlioglu et al. [49]. R123 is preferable to R152. Shet et al. [50] investigated an exergetic and  
169 energetic analysis of the CO<sub>2</sub> refrigeration system (transcritical mode) using an EES. Chen et al.  
170 [51] showed the thermal efficiency with R32 is slightly higher than that with the CO<sub>2</sub> system. An ORC  
171 device with maximum power output as an objective feature was considered by Oyewumni et al. [52]. A  
172 system by Cayer et al. [53] running on a Rankine transcritical cycle draws larger power to the (simple)  
173 subcritical cycle. The ratio of the evaporator to the  $P_{crit}$  for corresponding ORC fluid should lie in the  
174 range of 4 to 5 to achieve this result. Rawat et al. [54] focused on the energy crisis as a serious problem  
175 faced across the globe because of an increase in the day-by-day population which directly and indirectly  
176 hampers the environment and the economy. Aphornratana et al. [55] used heat at roughly 60 °C low-grade  
177 thermal energy employing R22 and R134a as refrigerants, the output of this integrated system produces a  
178 cooling effect at roughly -10 °C, and the coefficient of performance climbs from 0.1 to 0.6. Saleh  
179 [56] suggested that R602 emerges as the most significant fluid for the integrated system for the  
180 temperature range of 70 to 110 °C, out of 14 various refrigerants investigated. Malwe et al. [57] showed  
181 that R123 and R450a refrigerants are the best performing pair for the VCRES and ORC systems,  
182 respectively. The combined system's COP rises to 3.88 (compared to 3.17) with an overall exergy  
183 efficiency of roughly 18 % when ORC is used instead of a basic refrigeration system. Moles et al.  
184 [58] suggested that the combined system's thermal COP rises from 0.7 to 1.10 when the ORC-VCRES  
185 temperature rises and the condenser temperature falls. Over the other refrigerants, R1234ze(E) produces  
186 the best results. Wang et al. [59], [60] created a prototype with a 5-kW refrigeration capacity. The  
187 refrigerating effect and COP obtained in the experiments were 4.4 kW and 0.48, respectively. Kim et al.  
188 [61] have constructed a cogeneration plant employing low-grade heat energy as input to the system. Asim  
189 et al. [62] and Imran et al. [63] carried out energy, exergy and economic analysis of a combined VCRES  
190 and ORC called integrated air conditioning Organic Rankine Cycle system using 36 various sets of  
191 refrigerants. Asim et al. [64] evaluated a unique VCRES-ORC waste heat recovery system for tapping  
192 condenser heat of around 50 °C. The system under consideration has a refrigerating capacity of 35 kW.  
193 R600a-R141b produces the highest results (thermal efficiency = 3.05 %) and is the best choice for an  
194 integrated system. When ORC is used as part of an integrated VCRES-ORC system, the COP is 12.5 %  
195 greater than when utilizing a conventional VCRES system.

196 From the extensive literature survey done, it is found that most of the researchers have carried out the  
197 static simulations on the integrated VCRS-ORC system with only a few refrigerants considered for the  
198 research. This may be due to the limitations of the software used for simulation purposes. The necessity  
199 to perform this research work is to investigate the novel integration of a Vapor Compression  
200 Refrigeration System (VCRS) to an Organic Rankine Cycle (ORC) for low-grade waste heat recovery for  
201 improving the overall VCRS system efficiency. This creates a necessity to carry out research work on  
202 more refrigerants, with a larger number of VCRS-ORC refrigerant combinations, and that too with  
203 dynamic simulations.

### 204 1.3. *Novelties of the research work*

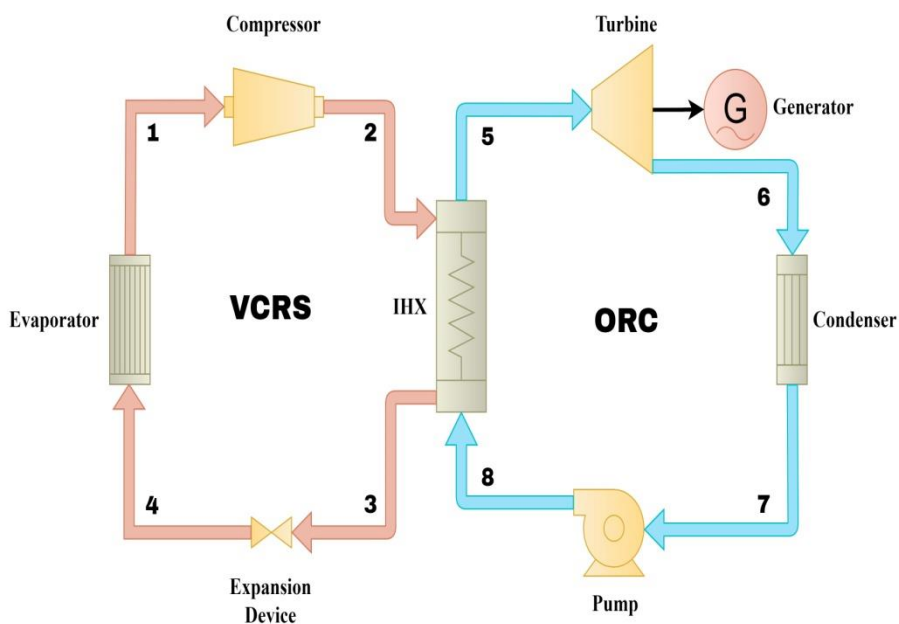
205 To analyze the integrated VCRS-ORC system, a custom model of the system was built on MATLAB-  
206 Simulink and refrigerant properties were imported from the Coolprop database. This methodology  
207 allowed the authors to perform a dynamic analysis of the system for varying VCRS evaporator  
208 temperature, VCRS load, and VCRS condenser temperature for 150 combinations of different refrigerant  
209 types. Dynamic simulations with MATLAB-Simulink and Coolprop database allow for the incorporation  
210 of 150 combinations of the simulation results. This is unlike the other research works using EES or  
211 MATLAB to simulate systems, which have limited capabilities in terms of dynamic analysis and the  
212 number of refrigerants selected for the analysis. The model developed for the dynamic simulation and  
213 performance assessment of the integrated VCRS-ORC system is verified with the [64] research paper.

214 The objective of this study is to perform both – the energy and exergy analysis of the VCRS-ORC  
215 system for all the 150 combinations of selected refrigerants. In conclusion in this research work, the  
216 authors found that for a VCRS-ORC integrated system, the refrigerant R1234ze(Z) in VCRS and R141b  
217 in ORC have minimal energy and exergy destruction and will be the best combination for this integrated  
218 system. The authors also found from the system dynamic analysis that, work output from ORC can be  
219 maximized by decreasing VCRS condenser temperature and increasing VCRS load. Decreasing VCRS  
220 condenser load is also found to decrease overall system exergy destruction.

## 221 2. System Description

222 The integrated VCRS-ORC system is divided into two parts, the VCRS part and the ORC part. The  
223 ORC part also consists of four major components, evaporator, expander, condenser, and pump. The  
224 working fluid recovers the low-grade waste heat from the condenser of VCRS, making it increase its  
225 enthalpy. This energy is recovered in the expander by making the high pressure and high temperature  
226 working fluid expand and generate power. This low-pressure working fluid is then condensed in the  
227 condenser and pumped back to high pressure in the pump to complete the ORC cycle. The schematic of

228 the integrated ORC-VCRS system is shown in Fig. 3(a) and the T-S diagram of the VCRS and ORC  
 229 systems is shown in Fig. 3(c) and Fig. 3 (d) respectively. Working fluid selection for both VCRS and  
 230 ORC systems is a crucial factor for this research work since the properties of working fluid will define the  
 231 energy and exergy efficiencies of the system as well as have significant importance in figuring out the  
 232 safety and environmental impact of the integrated VCRS-ORC system. For this research work, we have  
 233 considered 19 working fluids, selected following their feasibility with the system, availability, and  
 234 environmental impact. We have also selected some new and less researched working fluids to compare  
 235 their performance on the system against conventional working fluids. All 19 fluids are enlisted in Table 1  
 236 with their properties, safety, and environmental impact factors. A total of 10 working fluids were  
 237 considered for VCRs and 15 working fluids were considered for ORC. The fluids labeled as VCRS/ORC  
 238 in the table were used in both VCRS and ORC systems. Table 2 summarizes the physical, and  
 239 environmental properties of 20 refrigerants considered for the performance analysis and dynamic  
 240 simulation of the integrated VCRS-ORC system.



(a)

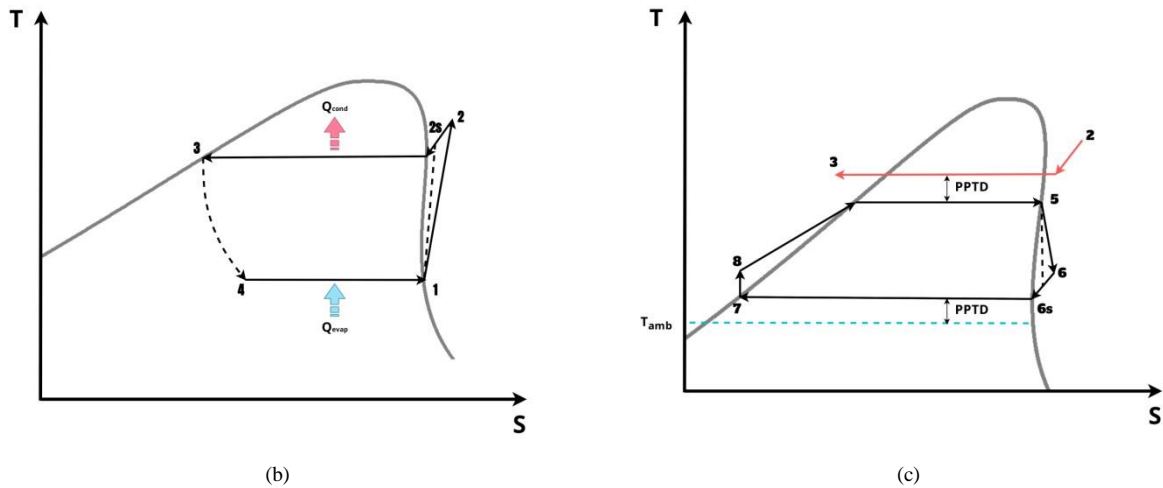


Fig. 3. (a) Schematic of the integrated VCRS-ORC system (b) T-s chart for the VCRS (c) T-s chart for the ORC system

### 3. Mathematical Model

The mathematical model for dynamic simulation and performance assessment of an integrated VCRS-ORC system is developed on MATLAB-Simulink (R2021a), with a fluid property database being imported from Coolprop [65]. The thermal analysis of the integrated system involves both energy and exergy analyses. This section presents all the energy and exergy equations used for the simulation model. However, for the ease of simulation and simplicity of the model, the following assumptions are considered:

#### 3.1. Assumptions

- Frictional, heat, kinetic, and potential energy losses and pressure drops across individual components are neglected.
- For the VCRS system, the refrigerant enters the compressor in a dry-saturated state and exits the condenser in a wet-saturated state.
- The throttling process in the expansion device of the VCRS system is considered to be isenthalpic.
- For the ORC system, refrigerant exits the turbine in a dry-saturated state and enters the pump in a wet-saturated state [4].

#### 3.2. Parameters considered

The parameters considered for performing energy and exergy analysis of the VCRS, ORC, and integrated VCRS-ORC system include various COPs ( $COP_{VCRS}$  and  $COP_{net}$ ), thermal efficiency ( $\eta_{th}$ ), component-wise and overall system exergy destruction ( $Ex_{dest}$ ), various exergy efficiencies ( $\eta_{ex,vcrs}$ ,  $\eta_{ex,orc}$ ,  $\eta_{ex,net}$ ).

### 3.3. Energy and exergy analysis

The energy analysis is carried out using the principles of the first law of thermodynamics. For the VCRS and ORC systems, calculating the  $COP_{vcrs}$  and  $\eta_{th}$  is the ultimate aim of the energy analysis. The energy analysis is based on the fundamentals of the second law of thermodynamics (eq. 1 and eq. 2).  $\eta_{ex,vcrs}$  and  $\eta_{ex,orc}$  are the final expected outcomes using the same. For the integrated VCRS-ORC system,  $COP_{net}$ , and  $\eta_{ex,net}$  are calculated. The formulation for the same is tabulated in Table 3:

Specific exergy flow of a component is given by [5]:

$$ex = (h - h_0) - T_0(s - s_0) \quad (1)$$

The general exergy balance in rate form: [16]:

$$\sum_{in} \left(1 - \frac{T_0}{T_i}\right) \dot{Q}_i + \dot{W}_{in} + \sum_{in} \dot{m}_i ex_i = \sum_{out} \left(1 - \frac{T_0}{T_i}\right) \dot{Q}_i + \dot{W}_{out} + \sum_{out} \dot{m}_i ex_i + \dot{E}x_D \quad (2)$$

Table 1. Operating conditions of the system

Parameter	Units	Value
Load on the evaporator	TR	1
Ambient temperature	°C	25
Evaporator temperature	°C	0
Condenser temperature	°C	45
Compressor isentropic efficiency	%	70
ORC pump isentropic efficiency	%	80
ORC turbine isentropic efficiency	%	80
Effectiveness of IHX	---	0.75
Pinch point temperature difference	°C	5

Table 2. Properties of the working fluids/refrigerants considered for the simulation and performance assessment of the integrated VCRS-ORC system

System	Refrigerant Group	Refrigerant Name	Refrigerant Type	Molecular mass (M) (kg/mol)	Critical temperature (T <sub>cr</sub> ) (°C)	Critical Pressure (P <sub>cr</sub> ) (bar)	ODP	GWP (for 100 years)	ASHRAE Safety	ASHRAE Flammability	ASHRAE Toxicity
VCRS	HCFC	R22	Wet	0.0864	96.29	49.9	0.055	1760	A1	Non-Flammable	Lower Toxicity
VCRS	HC	R290	Wet	0.0440	96.7	42.48	0	3.3	A3	Higher Flammability	Lower Toxicity
VCRS	HFC	R407C	Wet	0.0862	86.05	46.34	0	1774	A1	Non-Flammable	Lower Toxicity
VCRS	HFO	R1234ze(Z)	Dry	0.1140	150.27	35.30	0	6	A2L	Lower Flammability	Lower Toxicity
ORC	HCFC	R123	Isentropic	0.1529	183.68	36.62	0.02	79	B1	Non-Flammable	Higher Toxicity
ORC	HCFC	R141b	Isentropic	0.1169	204.2	42.50	0.12	725	A2	Lower Flammability	Lower Toxicity
ORC	HFC	R227ea	Dry	0.1700	102.8	29.80	0	3350	A1	Non-Flammable	Lower Toxicity
ORC	HFC	R245fa	Dry	0.1340	154.05	36.40	0	858	B1	Non-Flammable	Higher Toxicity
ORC	HFO	R1233zd(E)	Dry	0.1304	166.6	36.23	0	1	A1	Non-Flammable	Lower Toxicity
ORC	HFC	R245ca	Dry	0.1340	174.42	39.25	0	716	B1	Non-Flammable	Higher Toxicity
ORC	HCFC	R124	Dry	0.1364	122.28	36.24	0.02	527	A1	Non-Flammable	Lower Toxicity
ORC	HFC	R152a	Wet	0.0660	113.26	45.17	0	138	A2	Lower Flammability	Lower Toxicity
ORC	HFC	R32	Wet	0.0520	78.11	57.82	0	677	A2L	Lower Flammability	Lower Toxicity
VCRS/ORC	HFC	R134a	Isentropic	0.1020	101.21	40.59	0	1300	A1	Non-Flammable	Lower Toxicity
VCRS/ORC	HFC	R404A	Wet	0.0976	72.14	37.35	0	3922	A1	Non-Flammable	Lower Toxicity
VCRS/ORC	HC	R600a	Dry	0.0581	134.7	36.40	0	3	A3	Higher Flammability	Lower Toxicity
VCRS/ORC	HFC	R410A	Wet	0.0725	70.17	47.70	0	2088	A1	Non-Flammable	Lower Toxicity
VCRS/ORC	HFO	R1234ze(E)	Dry	0.1140	109.52	36.34	0	6	A2L	Lower Flammability	Lower Toxicity
VCRS/ORC	HFO	R1234yf	Dry	0.1140	94.85	33.82	0	4	A2L	Lower Flammability	Lower Toxicity

Table 3. Formulae used for energy and exergy analysis for the integrated VCRS-ORC system [64], [5], [16]

Energy Analysis		Exergy Analysis		
Compressor	$h_2 = \left(\frac{h_{2s} - h_1}{\eta_{is}}\right) + h_1$ (3)	Compressor	$Ex_{comp} = m_{vcrs}[(h_1 - h_2) - T_0(s_1 - s_2)] - W_{comp}$ (18)	
	$W_{comp} = m_{vcrs}(h_2 - h_1)$ (4)			
Condenser	$Q_{vcrs,cond} = m_{vcrs}(h_2 - h_3)$ (5)	Condenser	$Ex_{vcrs,cond} = (m_{vcrs}[(h_2 - h_3) - T_0(s_2 - s_3)] + (m_{orc}[(h_8 - h_5) - T_0(s_8 - s_5)]))$ (19)	
VCRS		Expansion valve	$Ex_{exp} = m_{vcrs}[(h_3 - h_4) - T_0(s_3 - s_4)]$ (20)	
	Evaporator	$Q_{vcrs,evap} = m_{vcrs}(h_1 - h_4)$ (6)	Evaporator	$Ex_{vcrs,evap} = (m_{vcrs}[(h_4 - h_1) - T_0(s_4 - s_1)] - \left(\left(1 - \frac{T_0}{T_4}\right)Q_{vcrs,evap}\right))$ (21)
COP	$COP_{vcrs} = \frac{Q_{vcrs,evap}}{W_{comp}}$ (7)	Exergy destruction	$Ex_{vcrs} = Ex_{comp} + Ex_{vcrs,cond} + Ex_{exp} + Ex_{vcrs,evap}$ (22)	
		Exergy efficiency	$\eta_{ex,vcrs} = 1 - \left(\frac{Ex_{vcrs}}{W_{comp}}\right)$ (23)	
Mass flow rate	$m_{orc} = \left(\frac{Q_{vcrs,cond} \cdot \epsilon_{hx}}{h_1 - h_4}\right)$ (8)	Evaporator	$Ex_{orc,evap} = (m_{orc}[(h_8 - h_5) - T_0(s_8 - s_5)] + (m_{vcrs}[(h_2 - h_3) - T_0(s_2 - s_3)]))$ (24)	
Evaporator	$Q_{orc,evap} = m_{orc}(h_5 - h_8)$ (9)			
Turbine	$h_6 = h_5 - [(h_5 - h_{6s}) \cdot \eta_{is}]$ (10)	Turbine	$Ex_{turb} = m_{orc}[(h_5 - h_6) - T_0(s_5 - s_6)] + W_{turb}$ (25)	
	$W_{turb} = m_{orc}(h_5 - h_6)$ (11)			
Pump	$h_8 = \left(\frac{h_{8s} - h_7}{\eta_{is}}\right) + h_7$ (12)	Pump	$Ex_{pump} = m_{orc}[(h_7 - h_8) - T_0(s_7 - s_8)] - W_{pump}$ (26)	
ORC				
	Condenser	$Q_{orc,cond} = m_{orc}(h_6 - h_7)$ (14)	Condenser	$Ex_{orc,cond} = (m_{orc}[(h_6 - h_7) - T_0(s_6 - s_7)] + \left(\left(1 - \frac{T_0}{T_7}\right)Q_{orc,cond}\right))$ (27)
Net work	$W_{net} = W_{turb} - W_{pump}$ (15)	Exergy destruction	$Ex_{orc} = Ex_{orc,evap} + Ex_{turb} + Ex_{pump} + Ex_{orc,cond}$ (28)	
Thermal Efficiency	$\eta_{th} = \frac{W_{turb}}{Q_{orc,evap}}$ (16)	Exergy efficiency	$\eta_{ex,orc} = \frac{W_{net}}{m_{vcrs}[(h_2 - h_3) - T_0(s_2 - s_3)]}$ (29)	
Integrated VCRS-ORC system	Net COP	$COP_{net} = \frac{Q_{vcrs,evap}}{W_{comp} - W_{net}}$ (17)	Overall/net exergy destruction	$Ex_{net} = Ex_{vcrs} + Ex_{orc}$ (30)
			Overall/net exergy efficiency	$\eta_{ex,net} = \frac{Q_{vcrs,evap} \left(1 - \frac{T_0}{T_4}\right)}{W_{comp} - W_{net}}$ (31)

### 3.4. Dynamic simulation model

In this research work, a dynamic simulation model of the integrated VCRS-ORC system is developed to analyze the system over a comprehensive range of input conditions and to scale up the number of working fluids being studied. This simulation model is developed on MATLAB-Simulink, enabling us to use its time step feature for dynamically simulating the system. To calculate working fluid properties during the simulation of different states, this model is integrated with Coolprop open-source database.

The simulation model is mainly divided into three parts, the VCRS model, ORC model, and energy and exergy analysis model. The simulation starts with the VCRS model, where first the VCRS working fluid is defined, followed by the calculation of its state points for the respective input conditions. This data is forwarded to the ORC model, where its state points for its respective input conditions are calculated. Finally, all the calculated state points data are forwarded to the final energy and exergy analysis model, where all equations from Table 3 are used to perform component-wise energy and exergy analysis.

To simulate multiple fluids at once, we have implemented a matrix type calculation layout for the model, where instead of calculating for one fluid at an instance, the model calculates state properties of all the considered fluids at once and stores the data of each fluid in specially allotted locations for that data in a matrix. To interact with data of another state matrix, the model uses matrix rules to perform mathematical operations. This approach allowed us to study much more working fluids than previously done. For a fixed ORC working fluid, the performance assessment of the integrated VCRS-ORC system using exergy analysis as a tool is done for 10 different VCRS refrigerants (R22, R134a, R290, R404A, R407C, R600a, R410A, R1234ze(E), R1234ze(Z), and R1234yf), and all the performance parameters like  $COP_{vcrs}$ ,  $COP_{net}$ ,  $W_{turb}$ ,  $Ex_{net}$ , and various exergy efficiencies are calculated individually for a particular VCRS refrigerant. So, for one ORC working fluid and for 10 VCRS refrigerants, 10 sets of the results are obtained. This process is repeated for 15 corresponding ORC fluids (R600a, R123, R141b, R227ea, R245fa, R1234ze(E), R134a, R245ca, R124, R152a, R404A, R410A, R32, R1233zd(E), and R1234yf). Consequently, 150 (15 ORC refrigerants  $\times$  10 VCRS refrigerants) sets of the results are obtained for the above said ORC-VCRS refrigerant combinations.

For dynamically simulating the model, input parameters vary linearly over a range and magnitudes of these parameters were stepped through this range by Simulink to have a dynamic image of the model. In this research work, VCRS evaporator temperature, VCRS condenser temperature, and load on VCRS were varied over a range of  $0^{\circ}\text{C} - 10^{\circ}\text{C}$ ,  $45^{\circ}\text{C} - 60^{\circ}\text{C}$ , and 1 TR – 10 TR respectively for all the considered working fluids. Fig. 4 shows the general flow process of the dynamic simulation model. The input parameters are depicted in orange color. VCRS model takes in  $T_1$ ,  $T_3$ ,  $Q_{evap}$ , and  $\eta_{is}$  as input

308 parameters to calculate state -1 to state - 4. The VCRS model gives  $m_{\text{vcrs}}$  as its output, and it is used along  
309 with PPTD,  $T_3$ ,  $T_{\text{amb}}$ ,  $\eta_{\text{is}}$ , and  $e_{\text{hx}}$  as input parameters for the ORC model. The outputs of both the VCRS  
310 and ORC models are used in the energy and exergy analysis model to calculate  $\text{COP}_{\text{net}}$ ,  $W_{\text{net}}$ ,  $\eta_{\text{th}}$ ,  $\text{COP}_{\text{net}}$ ,  
311  $\eta_{\text{ex}}$ , and  $\text{Ex}_{\text{net}}$ .

### 312 3.5. Model verification

313 The integrated VCRS-ORC system dynamic simulation model is verified with the model in the  
314 research work of [64]. For verification, similar input parameters present in the above-said research work  
315 were replicated in the current model and the obtained results were compared. The VCRS working fluid is  
316 considered R22 for the model verification with all VCRS input parameters listed in Table 4.

317 Fig. 5 (a), (b), and (c) show the model verification between the present study and research work by  
318 [64]. The verification is done by varying the condenser temperature for calculating the corresponding  
319 variation in the compressor work,  $\text{COP}_{\text{vcrs}}$ , and refrigerating effect. The verification results reveal that the  
320 percentage error between the present study and research work referred for compressor work,  $\text{COP}_{\text{vcrs}}$ , and  
321 refrigerating effect are 7.28 %, 12.76 %, and 0.09 % respectively. Since the performance curves show  
322 similar trends to that of referred work with a considerable deviation, the model is said to be verified for  
323 this study.

324 Table 4 . VCRS model validation input parameters [64]

VCRS Parameters	Values
Evaporator temperature	-20 °C
Condenser temperature	30 °C to 70 °C
Compressor isentropic efficiency	0.7
Pinch point temperature difference	5 °C

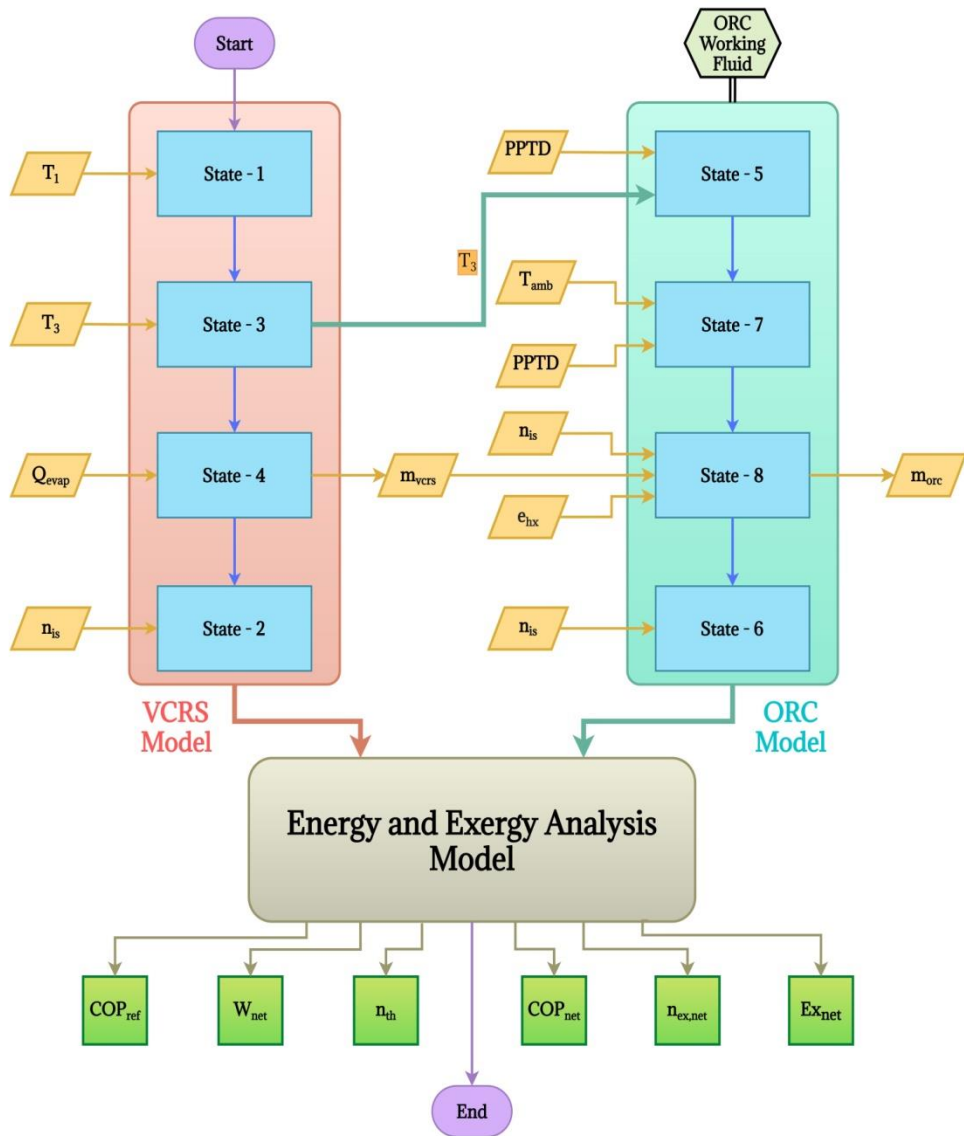
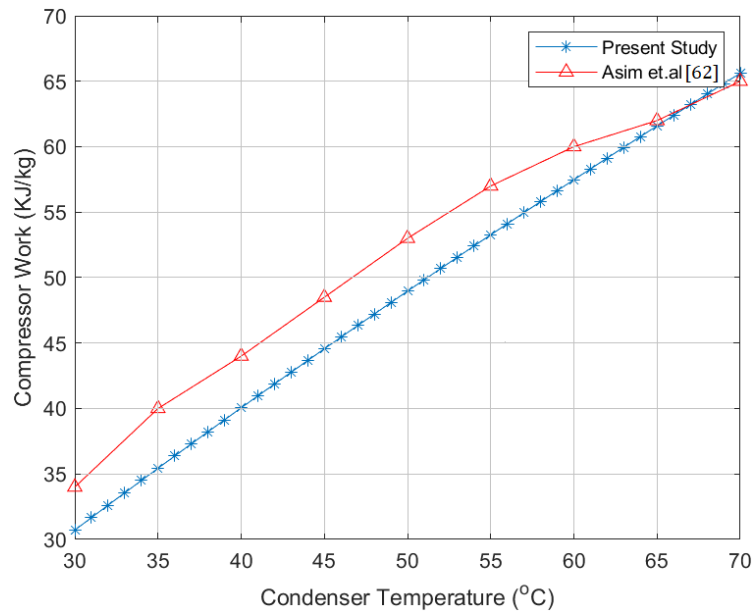
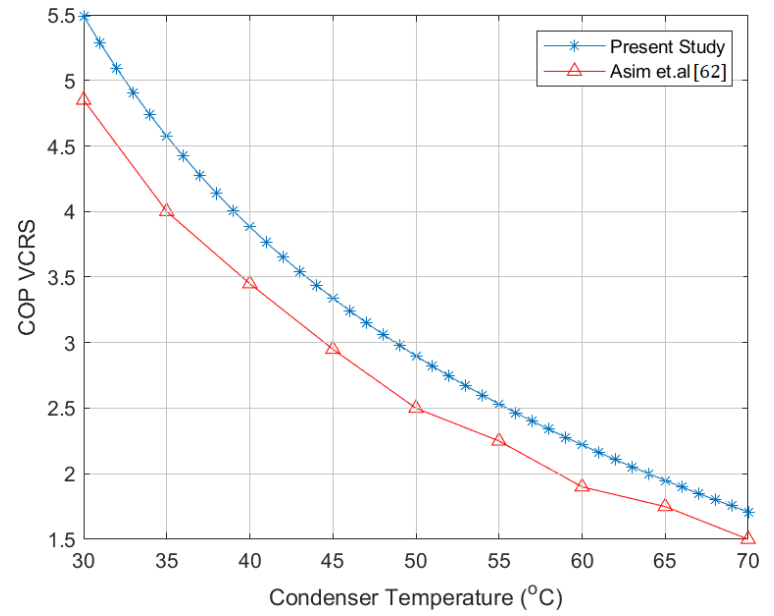


Fig. 4. Flow chart for the dynamic simulation of the integrated VCRES-ORC system

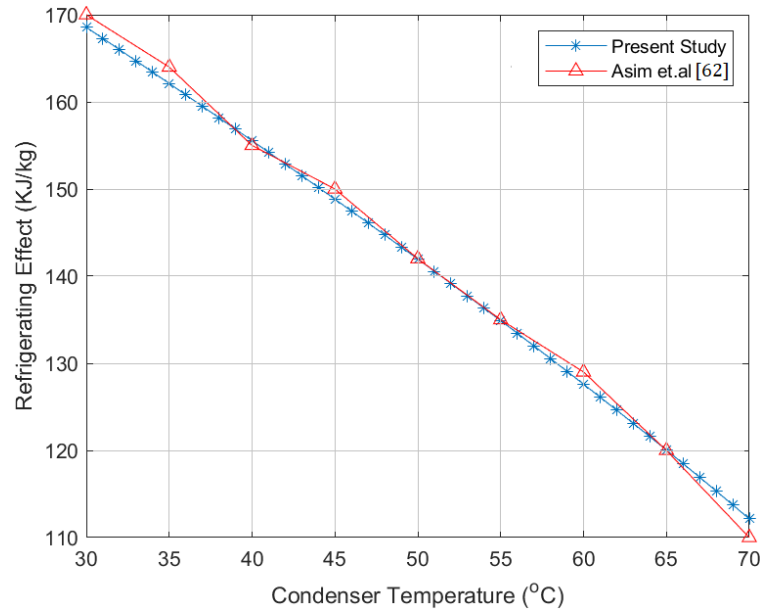
325  
326  
327  
328



(a)



(b)



(c)

Fig. 5. Model verification between the present study and a reference paper by varying the condenser temperature for the variation in (a) compressor work (b) COP of VCERS (c) refrigerating effect

## 4. Results and Discussions

This section deals with the simulation results followed by the discussions using various graphs for the performance analysis of the integrated VCRS-ORC systems. For the simulation purpose, Table 5 gives the values of the various performance parameters like COP, turbine work output, exergy efficiency, and exergy destructions for the corresponding set of refrigerant combinations. The dynamic simulation is performed for the specific set of conditions as mentioned in Table 5. A total of 20 refrigerants are considered for the dynamic simulation of the integrated vapor compression refrigeration system - Organic Rankine Cycle system. For a fixed ORC working fluid, 10 different VCRS refrigerants (R22, R134a, R290, R404A, R407C, R600a, R410A, R1234ze(E), R1234ze(Z), and R1234yf) are used for the analysis. This process is repeated for 15 corresponding ORC fluids (R600a, R123, R141b, R227ea, R245fa, R1234ze(E), R134a, R245ca, R124, R152a, R404A, R410A, R32, R1233zd(E), and R1234yf). Consequently, 150 sets of the results are obtained for the above said ORC-VCRS refrigerant combinations. In comparison to all ORC-VCRS refrigerants combinations, the best performance is obtained for the R141b – R1234ze(Z) pair as the ORC and VCRS refrigerant respectively. All the performance parameters for this combination gives maximum values ( $COP_{vcrs} = 4.152$ ,  $COP_{net} = 4.593$ ,  $\dot{\eta}_{ex,vcrs} = 29.871\%$ , and  $\dot{\eta}_{ex,net} = 33.045\%$ ); whereas the least exergy destruction ( $Ex_{net} = 2.591$  kW) is obtained for this combination. For this reason, various performance graphs are plotted and discussed for the R141b – R1234ze(Z) pair only.

From Table 5, among the different ORC-VCRS refrigerants combinations, the best performance in comparisons among the allis obtained for the R141b–R1234ze(Z) combination as the ORC and VCRS refrigerant respectively. The reason being for the R141b–R1234ze(Z) combination, all the performance parameters maximum values are obtained ( $COP_{vcrs} = 4.152$ ,  $COP_{net} = 4.593$ ,  $\dot{\eta}_{ex,vcrs} = 29.871\%$ , and  $\dot{\eta}_{ex,net} = 33.045\%$ ). This combination shows the least  $Ex_{net}$  of 2.591 kW among the all. Due to these reasons, the R141b – R1234ze(Z) combination is considered the best performance pair, and the various performance graphs are plotted and discussed as shown below.

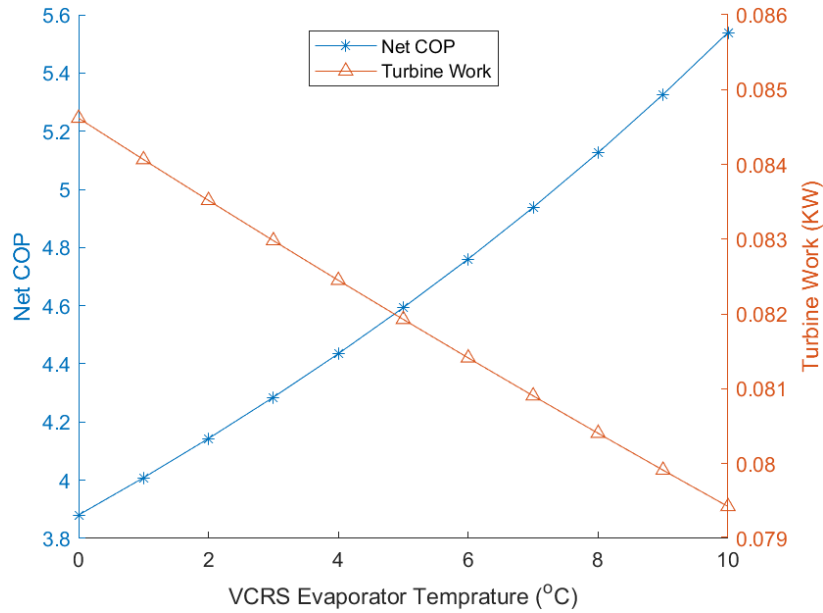
Table 5. Performance analysis of the integrated VCRS-ORC system for different sets of refrigerant combinations

Sr. No.	ORC working fluid	VCRS working fluid	COP <sub>vers</sub>	COP <sub>net</sub>	W <sub>turb</sub> (kW)	$\dot{\eta}_{th,orc}$ (%)	$\dot{\eta}_{ex,vers}$ (%)	$\dot{\eta}_{ex,orc}$ (%)	Ex <sub>net</sub> (kW)	$\dot{\eta}_{ex,net}$ (%)
1.	R600a	R22	3.905	4.288	0.083	2.518	28.09	26.428	2.778	30.85
2.		R134a	3.866	4.242	0.084	2.518	27.812	28.22	2.76	30.52
3.		R290	3.787	4.15	0.084	2.518	27.246	28.209	2.807	29.853
4.		R404A	3.35	3.639	0.086	2.518	24.469	27.831	3.12	26.607
5.		R407C	3.229	3.499	0.087	2.518	27.199	24.092	3.343	30.831
6.		R600a	3.963	4.357	0.083	2.518	28.509	28.884	2.686	31.346
7.		R410A	3.547	3.868	0.085	2.518	25.554	25.917	3.013	27.932
8.		R1234ze(E)	3.842	4.214	0.084	2.518	27.64	28.774	2.759	30.318
9.		R1234ze(Z)	4.152	4.583	0.082	2.518	29.871	28.405	2.599	32.969
10.		R1234yf	3.642	3.979	0.085	2.518	26.203	28.874	2.881	28.627
11.	R123	R22	3.905	4.295	0.083	2.496	28.09	26.884	2.771	30.902
12.		R134a	3.866	4.249	0.083	2.496	27.812	28.707	2.753	30.572
13.		R290	3.787	4.156	0.083	2.496	27.246	28.696	2.8	29.902
14.		R404A	3.35	3.644	0.085	2.496	24.469	28.312	3.113	26.647
15.		R407C	3.229	3.504	0.086	2.496	27.199	24.508	3.335	30.876
16.		R600a	3.963	4.365	0.082	2.496	28.509	29.383	2.679	31.4
17.		R410A	3.547	3.874	0.084	2.496	25.554	26.364	3.006	27.976
18.		R1234ze(E)	3.842	4.221	0.083	2.496	27.64	29.271	2.752	30.368
19.		R1234ze(Z)	4.152	4.591	0.082	2.496	29.871	28.895	2.592	33.028
20.		R1234yf	3.642	3.985	0.084	2.496	26.203	29.372	2.874	28.672
21.	R141b	R22	3.905	4.298	0.083	2.503	28.09	27.018	2.77	30.917
22.		R134a	3.866	4.252	0.083	2.503	27.812	28.85	2.752	30.587
23.		R290	3.787	4.158	0.083	2.503	27.246	28.839	2.8	29.917
24.		R404A	3.35	3.646	0.086	2.503	24.469	28.453	3.112	26.659
25.		R407C	3.229	3.506	0.086	2.503	27.199	24.63	3.335	30.889
26.		R600a	3.963	4.367	0.083	2.503	28.509	29.529	2.678	31.416
27.		R410A	3.547	3.875	0.085	2.503	25.554	26.496	3.005	27.989
28.		R1234ze(E)	3.842	4.223	0.083	2.503	27.64	29.417	2.751	30.383
29.		R1234ze(Z)	4.152	4.593	0.082	2.503	29.871	29.039	2.591	33.045
30.		R1234yf	3.642	3.987	0.084	2.503	26.203	29.519	2.874	28.686
31.	R227ea	R22	3.905	4.277	0.083	2.508	28.09	25.748	2.784	30.772
32.		R134a	3.866	4.232	0.083	2.508	27.812	27.494	2.766	30.444
33.		R290	3.787	4.139	0.084	2.508	27.246	27.484	2.813	29.779
34.		R404A	3.35	3.631	0.086	2.508	24.469	27.116	3.126	26.549
35.		R407C	3.229	3.492	0.087	2.508	27.199	23.472	3.349	30.765
36.		R600a	3.963	4.346	0.083	2.508	28.509	28.142	2.692	31.266
37.		R410A	3.547	3.859	0.085	2.508	25.554	25.251	3.019	27.868
38.		R1234ze(E)	3.842	4.204	0.083	2.508	27.64	28.034	2.765	30.242
39.		R1234ze(Z)	4.152	4.57	0.082	2.508	29.871	27.674	2.604	32.881
40.		R1234yf	3.642	3.97	0.084	2.508	26.203	28.131	2.887	28.559
41.	R245fa	R22	3.905	4.292	0.083	2.491	28.09	26.695	2.772	30.88
42.		R134a	3.866	4.247	0.083	2.491	27.812	28.505	2.754	30.551
43.		R290	3.787	4.154	0.083	2.491	27.246	28.494	2.802	29.882
44.		R404A	3.35	3.642	0.085	2.491	24.469	28.113	3.114	26.631
45.		R407C	3.229	3.502	0.086	2.491	27.199	24.335	3.337	30.858
46.		R600a	3.963	4.361	0.082	2.491	28.509	29.176	2.68	31.378
47.		R410A	3.547	3.871	0.084	2.491	25.554	26.179	3.007	27.958
48.		R1234ze(E)	3.842	4.218	0.083	2.491	27.64	29.065	2.753	30.347
49.		R1234ze(Z)	4.152	4.587	0.082	2.491	29.871	28.692	2.593	33.003
50.		R1234yf	3.642	3.983	0.084	2.491	26.203	29.166	2.876	28.653

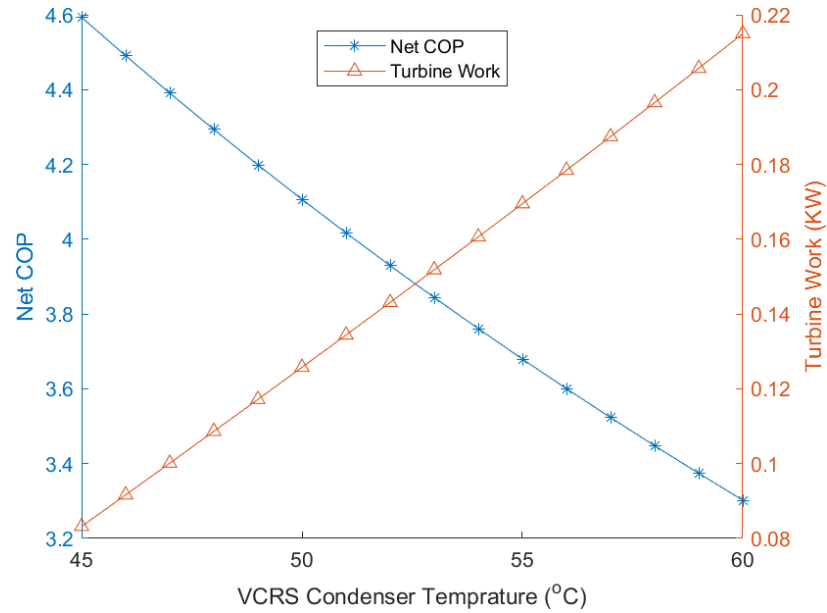
Sr. No.	ORC working fluid	VCRS working fluid	COP <sub>vers</sub>	COP <sub>net</sub>	W <sub>turb</sub>	$\dot{\eta}_{th,orc}$	$\dot{\eta}_{ex,vers}$	$\dot{\eta}_{ex,orc}$	EX <sub>net</sub>	$\dot{\eta}_{ex,net}$
51.		R22	3.905	4.284	0.084	2.53	28.09	26.182	2.782	30.821
52.		R134a	3.866	4.238	0.084	2.53	27.812	27.957	2.764	30.493
53.		R290	3.787	4.146	0.084	2.53	27.246	27.947	2.811	29.826
54.		R404A	3.35	3.636	0.087	2.53	24.469	27.572	3.124	26.586
55.	R1234ze(E)	R407C	3.229	3.496	0.087	2.53	27.199	23.868	3.347	30.807
56.		R600a	3.963	4.353	0.084	2.53	28.509	28.615	2.69	31.317
57.		R410A	3.547	3.864	0.086	2.53	25.554	25.676	3.017	27.909
58.		R1234ze(E)	3.842	4.21	0.084	2.53	27.64	28.506	2.763	30.29
59.		R1234ze(Z)	4.152	4.578	0.083	2.53	29.871	28.14	2.603	32.937
60.		R1234yf	3.642	3.976	0.085	2.53	26.203	28.605	2.885	28.602
61.		R22	3.905	4.283	0.084	2.549	28.09	26.12	2.784	30.814
62.		R134a	3.866	4.238	0.085	2.549	27.812	27.891	2.766	30.486
63.		R290	3.787	4.145	0.085	2.549	27.246	27.88	2.814	29.819
64.		R404A	3.35	3.635	0.087	2.549	24.469	27.507	3.127	26.581
65.	R134a	R407C	3.229	3.496	0.088	2.549	27.199	23.811	3.349	30.801
66.		R600a	3.963	4.352	0.084	2.549	28.509	28.547	2.693	31.31
67.		R410A	3.547	3.864	0.086	2.549	25.554	25.615	3.019	27.903
68.		R1234ze(E)	3.842	4.209	0.085	2.549	27.64	28.439	2.765	30.283
69.		R1234ze(Z)	4.152	4.577	0.083	2.549	29.871	28.073	2.605	32.929
70.		R1234yf	3.642	3.975	0.086	2.549	26.203	28.537	2.888	28.596
71.		R22	3.905	4.293	0.082	2.485	28.09	26.761	2.771	30.888
72.		R134a	3.866	4.248	0.082	2.485	27.812	28.576	2.753	30.558
73.		R290	3.787	4.155	0.083	2.485	27.246	28.565	2.8	29.889
74.		R404A	3.35	3.643	0.085	2.485	24.469	28.182	3.113	26.636
75.	R245ca	R407C	3.229	3.503	0.086	2.485	27.199	24.396	3.335	30.864
76.		R600a	3.963	4.363	0.082	2.485	28.509	29.248	2.679	31.385
77.		R410A	3.547	3.872	0.084	2.485	25.554	26.244	3.006	27.964
78.		R1234ze(E)	3.842	4.219	0.083	2.485	27.64	29.137	2.752	30.355
79.		R1234ze(Z)	4.152	4.589	0.081	2.485	29.871	28.763	2.592	33.012
80.		R1234yf	3.642	3.984	0.084	2.485	26.203	29.238	2.874	28.66
81.		R22	3.905	4.287	0.083	2.519	28.09	26.366	2.779	30.842
82.		R134a	3.866	4.241	0.084	2.519	27.812	28.154	2.761	30.513
83.		R290	3.787	4.149	0.084	2.519	27.246	28.143	2.808	29.846
84.		R404A	3.35	3.638	0.086	2.519	24.469	27.766	3.121	26.602
85.	R124	R407C	3.229	3.498	0.087	2.519	27.199	24.035	3.343	30.825
86.		R600a	3.963	4.356	0.083	2.519	28.509	28.816	2.687	31.339
87.		R410A	3.547	3.867	0.085	2.519	25.554	25.856	3.013	27.926
88.		R1234ze(E)	3.842	4.213	0.084	2.519	27.64	28.706	2.76	30.311
89.		R1234ze(Z)	4.152	4.582	0.082	2.519	29.871	28.338	2.599	32.961
90.		R1234yf	3.642	3.978	0.085	2.519	26.203	28.806	2.882	28.62
91.		R22	3.905	4.289	0.084	2.546	28.09	26.463	2.78	30.854
92.		R134a	3.866	4.243	0.085	2.546	27.812	28.258	2.762	30.524
93.		R290	3.787	4.15	0.085	2.546	27.246	28.247	2.81	29.856
94.		R404A	3.35	3.639	0.087	2.546	24.469	27.869	3.123	26.61
95.	R152a	R407C	3.229	3.5	0.088	2.546	27.199	24.124	3.345	30.835
96.		R600a	3.963	4.358	0.084	2.546	28.509	28.923	2.689	31.35
97.		R410A	3.547	3.868	0.086	2.546	25.554	25.952	3.015	27.936
98.		R1234ze(E)	3.842	4.215	0.085	2.546	27.64	28.812	2.762	30.321
99.		R1234ze(Z)	4.152	4.583	0.083	2.546	29.871	28.442	2.601	32.973
100.		R1234yf	3.642	3.98	0.086	2.546	26.203	28.912	2.884	28.63

Sr. No.	ORC working fluid	VCRS working fluid	COP <sub>vers</sub>	COP <sub>net</sub>	W <sub>turb</sub>	$\dot{\eta}_{th,orc}$	$\dot{\eta}_{ex,vers}$	$\dot{\eta}_{ex,orc}$	EX <sub>net</sub>	$\dot{\eta}_{ex,net}$
101.	R404A	R22	3.905	4.25	0.085	2.558	28.09	24.038	2.805	30.578
102.		R134a	3.866	4.205	0.085	2.558	27.812	25.668	2.787	30.254
103.		R290	3.787	4.114	0.085	2.558	27.246	25.658	2.835	29.597
104.		R404A	3.35	3.611	0.088	2.558	24.469	25.314	3.148	26.402
105.		R407C	3.229	3.473	0.088	2.558	27.199	21.913	3.371	30.6
106.		R600a	3.963	4.318	0.085	2.558	28.509	26.272	2.713	31.066
107.		R410A	3.547	3.836	0.087	2.558	25.554	23.573	3.04	27.706
108.		R1234ze(E)	3.842	4.178	0.085	2.558	27.64	26.172	2.786	30.054
109.		R1234ze(Z)	4.152	4.54	0.084	2.558	29.871	25.836	2.626	32.662
110.		R1234yf	3.642	3.946	0.086	2.558	26.203	26.262	2.909	28.389
111.	R410A	R22	3.905	4.262	0.088	2.643	28.09	24.806	2.807	30.665
112.		R134a	3.866	4.217	0.088	2.643	27.812	26.488	2.789	30.339
113.		R290	3.787	4.125	0.088	2.643	27.246	26.478	2.837	29.678
114.		R404A	3.35	3.62	0.091	2.643	24.469	26.124	3.15	26.467
115.		R407C	3.229	3.481	0.091	2.643	27.199	22.613	3.373	30.674
116.		R600a	3.963	4.331	0.087	2.643	28.509	27.112	2.715	31.156
117.		R410A	3.547	3.846	0.089	2.643	25.554	24.327	3.042	27.778
118.		R1234ze(E)	3.842	4.189	0.088	2.643	27.64	27.008	2.788	30.138
119.		R1234ze(Z)	4.152	4.554	0.087	2.643	29.871	26.661	2.628	32.76
120.		R1234yf	3.642	3.957	0.089	2.643	26.203	27.102	2.911	28.465
121.	R32	R22	3.905	4.276	0.088	2.648	28.09	25.692	2.799	30.765
122.		R134a	3.866	4.231	0.088	2.648	27.812	27.434	2.781	30.438
123.		R290	3.787	4.138	0.088	2.648	27.246	27.424	2.829	29.773
124.		R404A	3.35	3.63	0.091	2.648	24.469	27.056	3.142	26.544
125.		R407C	3.229	3.491	0.091	2.648	27.199	23.421	3.365	30.76
126.		R600a	3.963	4.345	0.087	2.648	28.509	28.08	2.707	31.259
127.		R410A	3.547	3.858	0.09	2.648	25.554	25.195	3.034	27.862
128.		R1234ze(E)	3.842	4.203	0.088	2.648	27.64	27.973	2.78	30.236
129.		R1234ze(Z)	4.152	4.569	0.087	2.648	29.871	27.614	2.62	32.874
130.		R1234yf	3.642	3.969	0.089	2.648	26.203	28.07	2.903	28.553
131.	R1233zd(E)	R22	3.905	4.294	0.083	2.496	28.09	26.791	2.772	30.891
132.		R134a	3.866	4.248	0.083	2.496	27.812	28.608	2.754	30.561
133.		R290	3.787	4.155	0.083	2.496	27.246	28.597	2.801	29.892
134.		R404A	3.35	3.643	0.085	2.496	24.469	28.214	3.114	26.639
135.		R407C	3.229	3.503	0.086	2.496	27.199	24.423	3.336	30.867
136.		R600a	3.963	4.363	0.082	2.496	28.509	29.281	2.68	31.389
137.		R410A	3.547	3.872	0.084	2.496	25.554	26.273	3.007	27.967
138.		R1234ze(E)	3.842	4.22	0.083	2.496	27.64	29.17	2.753	30.358
139.		R1234ze(Z)	4.152	4.589	0.082	2.496	29.871	28.795	2.593	33.016
140.		R1234yf	3.642	3.984	0.084	2.496	26.203	29.271	2.875	28.663
141.	R1234yf	R22	3.905	4.277	0.085	2.556	28.09	25.759	2.789	30.773
142.		R134a	3.866	4.232	0.085	2.556	27.812	27.506	2.771	30.445
143.		R290	3.787	4.139	0.085	2.556	27.246	27.495	2.818	29.781
144.		R404A	3.35	3.631	0.088	2.556	24.469	27.127	3.131	26.549
145.		R407C	3.229	3.492	0.088	2.556	27.199	23.482	3.354	30.766
146.		R600a	3.963	4.346	0.084	2.556	28.509	28.153	2.697	31.267
147.		R410A	3.547	3.859	0.086	2.556	25.554	25.261	3.024	27.869
148.		R1234ze(E)	3.842	4.204	0.085	2.556	27.64	28.045	2.77	30.243
149.		R1234ze(Z)	4.152	4.571	0.084	2.556	29.871	27.685	2.61	32.882
150.		R1234yf	3.642	3.97	0.086	2.556	26.203	28.143	2.893	28.56

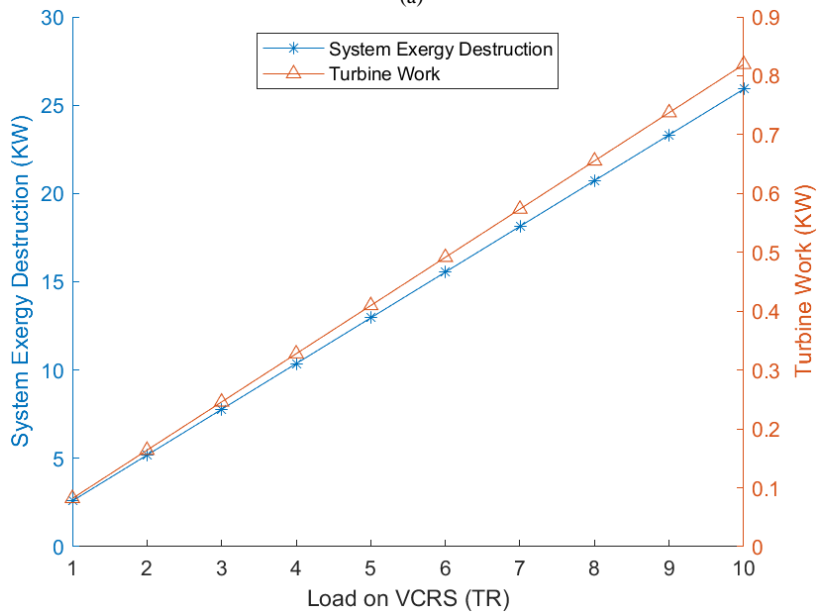
The best combination of refrigerant pair      Maximum value      Minimum value



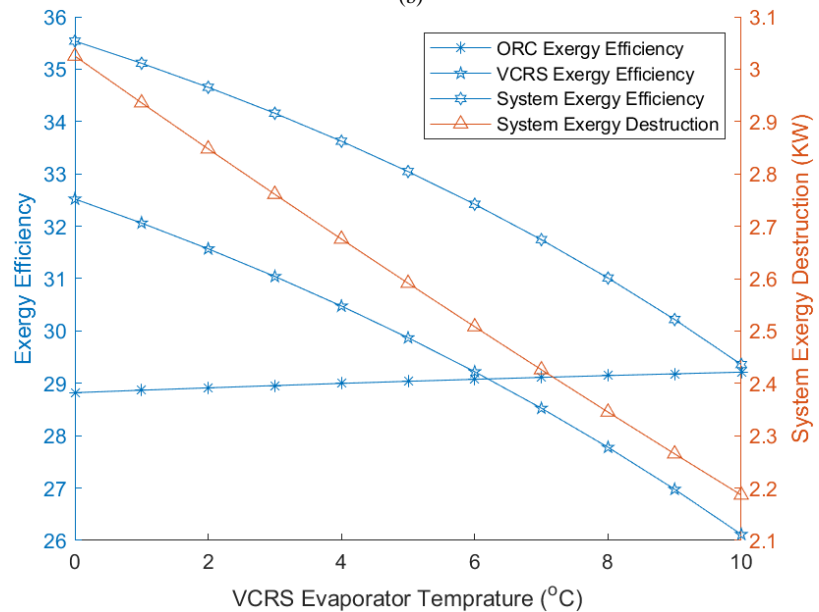
(a)



(b)



(c)



(d)

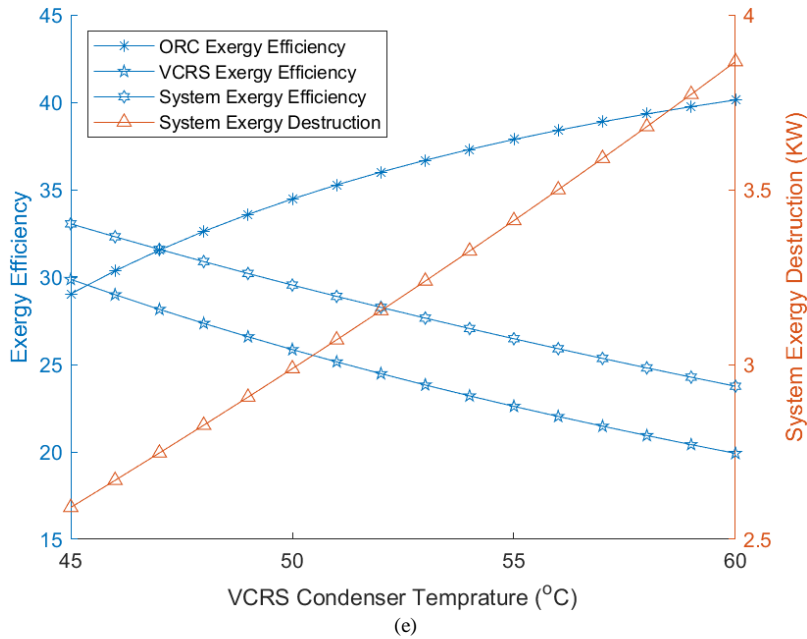


Fig. 6. (a) Variation of net COP and turbine work against the VCRS evaporator temperature (b) Variation of net COP and turbine work against the VCRS condenser temperature (c) Variation of system exergy destruction and turbine work against load on VCRS (d) Variation of exergy efficiencies of ORC, VCRS and combined system, and system exergy destruction against the VCRS evaporator temperature (e) Variation of exergy efficiencies of ORC, VCRS and combined system and system exergy destruction against the VCRS condenser temperature

The performance of the integrated VCRS-ORC system is further assessed using various performance curves among the calculated parameters. Fig. 6 (a) and (b) show the variation for net COP, and turbine work against the VCRS evaporator and condenser temperatures respectively. It is found that, with an increase in the VCRS evaporator temperature (varied from 0 °C to 10 °C), the net COP increases (from 3.9 to 5.5); the turbine work output of the ORC however decreases (from 84.5 W to 78.5 W) correspondingly. This is because net COP is proportional to the evaporator temperature and consequently it increases. Although, the net COP of the system decreases due to an increase in the VCRS evaporator temperature; thus, and the overall power reduces. Assuming the pump work constant, this causes a decrease in the turbine work power output. Exactly reverse trend/variation is shown by the net COP and ORC turbine work output for an increase in condenser temperature. With an increase in the VCRS condenser temperature (varied from 0 °C to 10 °C), the net COP decreases (from 4.6 to 3.3); the turbine work output of the ORC however increases (from 80 W to 220 W) correspondingly.

Fig. 6 (c) depicts the variation of the system exergy destruction and the ORC turbine work output by varying the load on the refrigeration system. The results reveal that, as the load increases (from 1 TR to 10 TR), both – the system exergy destruction and the ORC turbine work output linearly increase from 2.5 kW to 25 kW, and 0.1 kW to 0.8 kW respectively. At higher loads, higher entropy generation takes place inside the system, which reduces the exergy potential due to the exergy destruction. However, the net COP of the system increases correspondingly, which causes an increase in the ORC turbine work output.

382 Fig. 6 (d) shows the variation of exergy efficiencies of ORC, VCRS, and combined system, and system  
383 exergy destruction against the VCRS evaporator temperature. For an increase in the VCRS evaporator  
384 temperature (from 0 °C to 10 °C), the VCRS, ORC, and overall integrated system exergy efficiencies  
385 decrease (from 32.5 % to 26 %), increases slightly (from 28.8 % to 29.2 %), and decreases (from 35.5 %  
386 to 29.5 %) respectively; the overall system exergy destruction, however, decreases from 3 kW to 2.2 kW.  
387 The VCRS exergy efficiency is indirectly proportional to the VCRS evaporator temperature. However, it  
388 does not affect to a considerable extent the ORC exergy efficiency and thus it shows a slight increase  
389 only. The system exergy efficiency is the combined effect of the above-two efficiencies.

390 Fig. 6 (e) shows the variation of the above-mentioned performance parameters with the variation in  
391 VCRS condenser temperature. For an increase in the VCRS condenser temperature (from 45 °C to 60 °C),  
392 the VCRS, ORC, and overall integrated system exergy efficiencies decrease (from 30 % to 22.5 %),  
393 increase (from 29 % to 39 %), and decreases (from 33 % to 26 %) respectively; the overall system exergy  
394 destruction, however, increases from 2.6 kW to 3.85 kW. Higher the condenser temperature, the higher  
395 the system exergy destruction takes place. Similar to the earlier curves, the VCRS exergy efficiency is  
396 indirectly proportional to the VCRS condenser temperature. However, it varies directly with the ORC  
397 exergy efficiency and thus it shows a linear increase. The system exergy efficiency is the combined effect  
398 of the above-two efficiencies.

## 399 5. Conclusion

400 This research work has performed a dynamic simulation and performance assessment of an integrated  
401 vapor compression refrigeration system - Organic Rankine Cycle system using the exergy analysis as a  
402 tool. The system taken under consideration includes a refrigeration system installed to produce a cooling  
403 effect and preserve the raisins. The waste heat rejected from the condenser of a refrigeration plant is  
404 utilized as a potential/input to drive an organic Rankine Cycle system. This system which is supposed to  
405 be installed is modeled for the corresponding input and operating conditions. The conclusion of the paper  
406 can be summarized as follows:

- 407 • From the performance graphs, with an increase in the VCRS evaporator temperature (varied from 0  
408 °C to 10 °C), the net COP increases (from 3.9 to 5.5), and the  $W_{\text{turb}}$  decreases (from 84.5 W to 78.5  
409 W) correspondingly. However, a reverse trend is shown by the net COP and ORC turbine work  
410 output for an increase in the condenser temperature. With an increase in the VCRS condenser  
411 temperature (varied from 0 °C to 10 °C), the net COP decreases (from 4.6 to 3.3), and the  $W_{\text{turb}}$   
412 increases (from 80 W to 220 W) correspondingly.

- 413 • As the load on the VCRS increases (from 1 TR to 10 TR), both –  $Ex_{net}$  and the  $W_{turb}$  linearly  
414 increase from 2.5 kW to 25 kW, and 0.1 kW to 0.8 kW respectively.
- 415 • For an increase in the VCRS evaporator temperature (from 0 °C to 10 °C), the exergy efficiencies  
416 for VCRS, ORC, and overall integrated system decrease (from 32.5 % to 26 %), increase slightly  
417 (from 28.8 % to 29.2 %), decreases (from 35.5 % to 29.5 %) respectively, and the  $Ex_{net}$  decreases  
418 from 3 kW to 2.2 kW.
- 419 • For an increase in the VCRS condenser temperature (from 45 °C to 60 °C), the exergy efficiencies  
420 for VCRS, ORC, and overall integrated system decrease (from 30 % to 22.5 %), increases (from 29  
421 % to 39 %), decrease (from 33 % to 26 %) respectively, and the overall  $Ex_{net}$  increases from 2.6 kW  
422 to 3.85 kW.

423 Hence, from this research work, it can be concluded that, for performing the waste heat recovery  
424 utilizing the heat rejected from the condenser of a VCRS (operating range 60 °C to 70 °C), R141b–  
425 R1234ze(Z) stands as the optimum ORC-VCRS refrigerant pair, considering the thermal performance and  
426 exergy assessment.

#### 427 **Acknowledgments**

428 The authors are thankful to the Director, HoD - Mechanical Engineering, and TEQIP-III officials of  
429 the Walchand College of Engineering, Sangli, for their encouragement and assistance. Also, grateful to  
430 the AICTE-NDF scheme officials, in New Delhi, India, for launching the scheme and giving such an  
431 excellent platform for conducting research.

#### 432 **Conflict of Interest**

433 The authors declare no conflict of interest.

#### 434 **Funding**

435 This research project received funding for the experimentation from the TEQIP III Seed Funding,  
436 Walchand College of Engineering, Sangli, Maharashtra, India. [Funding Grant/Ref. No.: *TEQIP III/*  
437 *SFOrder/1489*].

<i>Abbreviations</i>		<i>Greek Symbols</i>	
ORC	Organic Rankine Cycle	$\eta$	efficiency
VCRS	Vapor Compression Refrigeration System	$\epsilon$	effectiveness
TR	Tons of Refrigeration	<i>Subscripts</i>	
COP	Coefficient of Performance	cri	critical
AIDA	Analysis, Implement, Design, and Assessment	vcrs	vapor compression refrigeration system
GWP	Global Warming Potential	th	thermal
CFC	Chlorofluorocarbon	ex,vcrs	exergy of vapor compression refrigeration system
HCFC	Hydrochlorofluorocarbon	ex,orc	exergy of organic Rankine cycle
EU	European Union	net	net/overall
HVAC	Heating, Ventilation, and Air Conditioning	ex,net	net exergy efficiency
TEWI	Total Equivalent Warming Index	ex	exergy
EES	Engineering Equation Solver	0	dead state
ASHRAE	American Society for Heating, Ventilation, and Air Conditioning	in	inlet
IHX	Internal Heat Exchanger	i	i <sup>th</sup> state
ODP	Ozone Depletion Potential	out	outlet
HFO	Hydrofluoroolefin	D	destruction
MATLAB	Matrix Laboratory	s	saturated
TEQIP	Technical Education Quality Improvement Programme	comp	compressor
AICTE	All India Council for Technical Education	cond	condenser
NDF	National Doctoral Fellowship	evap	evaporator
<i>Parameters</i>		is	isentropic
P	Pressure	th	thermal
h	Enthalpy	turb	turbine
T	Temperature	exp	expansion device
s	Entropy		
Q	Heat		
W	Work		
m	Mass flow rate		
Ex	Exergy		

- [1] A. Mahmoudi, M. Fazli and M. R. Morad, "A recent review of waste heat recovery by Organic Rankine Cycle," *Applied Thermal Engineering*, vol. 143, pp. 660-675, 30 July 2018.
- [2] G. S. Wahile, P. D. Malwe and U. Aswalekar, "Latent heat storage system by using phase change materials and their application," *Materials Today: Proceedings*, pp. 1-7, 11 October 2021.
- [3] G. S. Wahile, P. D. Malwe and A. V. Kolhe, "Waste heat recovery from exhaust gas of an engine by using a phase change material," *Materials Today: Proceedings*, vol. 28, no. 4, pp. 2101-2107, 15 April 2020.
- [4] P. D. Malwe, B. Gawali, J. Shaikh, M. Deshpande, R. Dhalait, S. Kulkarni, V. Shindagi, H. Panchal and K. K. Sadasivuni, "Exergy assessment of an Organic Rankine Cycle for waste heat recovery from a refrigeration system: a review," *Chemical Engineering Communications*, pp. 1-29, 1 October 2021.
- [5] I. Dincer and M. A. Rosen, *Exergy: Energy, Environment and Sustainable Development*, 2nd ed., Amsterdam: Elsevier Ltd., 2012, p. 576.
- [6] I. Dincer, "Exergization," *International Journal of Energy Research*, vol. 40, pp. 1887-1889, 28 July 2016.
- [7] I. Dincer and T. A. Ratlamwala, "Importance of exergy for analysis improvement, design, and assessment," *WIREs Energy and Environment*, vol. 2, pp. 335-349, May 2013.
- [8] P. D. Malwe, B. S. Gawali and G. S. Wahile, "Exergy Analysis of a Four Stroke Diesel Engine," in *Techno-Societal 2018*, 1 ed., vol. 2, P. M. Pawar, B. P. Ronge, R. Balasubramaniam, A. S. Vibhute and S. S. Apte, Eds., Pandharpur, Maharashtra: Springer International Publishing, 2018, pp. 885-894.
- [9] P. D. Malwe, B. S. Gawali, M. S. Choudhari, R. S. Dhalait and N. S. Deshmukh, "Performance Analysis and Exergy Assessment of an Inertance Pulse Tube Cryocooler," *Journal of Thermal Engineering*, 2021.
- [10] J. U. Ahamed, R. Saidur and H. H. Masjuki, "A review on exergy analysis of vapor compression refrigeration system," *Renewable and Sustainable Energy Reviews*, vol. 15, no. 3, p. 1593-1600, 12 January 2011.
- [11] S. Anand, A. Gupta and S. K. Tyagi, "Simulation studies of refrigeration cycles: A review," *Renewable and Sustainable Energy Reviews*, vol. 17, pp. 260-277, 25 October 2012.
- [12] S. A. Borikar, M. M. Gupta, M. A. Alazawi, P. D. Malwe, E. B. Moustafa, H. Panchal and A. Elsheikh, "A case study on experimental and statistical analysis of energy consumption of domestic refrigerator," *Case Studies in Thermal Engineering* 28 (2021) 101636, vol. 28, pp. 1-10, 9 November 2021.
- [13] P. D. Malwe, B. S. Gawali and S. D. Thakre, "Exergy Analysis of Vapour Compression Refrigeration System," *International Journal of Thermal Technologies*, vol. 4, no. 2, pp. 54-57, 1 June 2014.
- [14] P. D. Malwe and B. S. Gawali, "Exergy Management of Vapour Compression Refrigeration System," *International Journal of Engineering Associates*, vol. 3, no. 1, pp. 33-36, 2014 March 2014.
- [15] P. D. Malwe, J. Shaikh and B. S. Gawali, "Exergy Assessment of a Multistage Multi-evaporator Vapor Compression Refrigeration System using Eighteen Refrigerants," *Energy Reports*, pp. 1-10, 10 November 2021.
- [16] R. B. Jemaa, R. Mansouri, I. Boukholda and A. Bellagi, "Energy and exergy investigation of R1234ze as R134a replacement in vapor compression chillers," *International Journal of Hydrogen Energy*, pp. 1-11, 03 December 2016.
- [17] A. M. Babiloni, J. M. Belman-Flores, P. Makhnatch, J. N. Esbri and J. M. Barroso-Maldonado, "Experimental exergy analysis of R513A to replace R134a in a small capacity refrigeration system," *Energy*, vol. 162, pp. 99-110, 04 August 2018.
- [18] A. E. Ozgur, A. Kabul and O. Kizilkan, "Exergy analysis of refrigeration systems using an alternative refrigerant (hfo-1234yf) to R-134a," *International Journal of Low Carbon Technologies Advance Access*, vol. 9, pp. 56-62, 17 May 2012.
- [19] A. Geete, M. Sharma and P. Shrimali, "Entropy generation and exergy destruction analyses for vapour compression refrigeration system with various refrigerants," *Springer Nature Applied Sciences*, vol. 764, no. 1, pp. 1-12, 22 June 2019.
- [20] R. Roy and B. K. Mandal, "Thermodynamic Analysis of Modified Vapour Compression Refrigeration System Using R-134a," *Energy Procedia*, vol. 109, pp. 227-234, March 2017.
- [21] G. and R. Kumar, "Computational energy and exergy analysis of R134a, R1234yf, R1234ze and their mixtures in vapour

- compression system," *Ain Shams Engineering Journal*, vol. 9, no. 4, p. 3229–3237, 13 November 2018.
- [22] N. D. Shikalgar and S. N. Sapali, "Energy and Exergy Analysis of a Domestic Refrigerator: Approaching a Sustainable Refrigerator," *Journal of Thermal Engineering*, vol. 5, no. 5, pp. 469-481, October 2019.
- [23] S. Agarwal, A. Arora and B. B. Arora, "Energy and Exergy Investigations of R1234yf and R1234ze as R134a Replacements in Mechanically Subcooled Vapour Compression Refrigeration Cycle," *Journal of Thermal Engineering*, vol. 7, no. 1, pp. 109-132, January 2021.
- [24] S. Kumar, M. Prevost and R. Bugarel, "Exergy analysis of a compression refrigeration system," *Heat Recovery Systems and CHP*, vol. 9, no. 2, pp. 151-157, 28 July 1988.
- [25] T. B. Fajar, R. P. Bagas, S. Ukhi, M. I. Alhamid and A. Lubis, "Energy and exergy analysis of an R410A small vapor compression system retrofitted with R290," *Case Studies in Thermal Engineering*, vol. 21, 31 May 2020.
- [26] A. Arora and S. C. Kaushik, "Theoretical analysis of a vapour compression refrigeration system with R502, R404A and R507A," *International Journal of Refrigeration*, vol. 31, no. 6, pp. 998-1005, 10 January 2008.
- [27] A. Yataganbaba, A. Kilicarslan and I. Kurtbas, "Exergy analysis of R1234yf and R1234ze as R134a replacements in a two evaporator vapour compression refrigeration system," *International Journal of Refrigeration*, vol. 60, pp. 26-37, 13 August 2015.
- [28] C. Nikolaidis and D. Probert, "Exergy-method analysis of a two-stage vapour-compression refrigeration-plants performance," *Applied Energy*, vol. 60, no. 4, pp. 241-256, 1 August 1998.
- [29] A. Anjum, M. Gupta, N. A. Ansari and R. S. Mishra, "Thermodynamic Analysis of a Two Stage Vapour Compression Refrigeration System Utilizing the Waste Heat of the Intercooler for Water Heating," *Journal of Fundamentals of Renewable Energy and Applications*, vol. 7, pp. 232-238, 21 July 2017.
- [30] M. M. Dwinanto, Suhanan and P. Prajitno, "Exergy analysis of a dual-evaporator refrigeration systems," in *AIP Conference Proceedings, International Conference on Engineering, Science and Nanotechnology*, Solo, 2017.
- [31] S. Quoilin, M. V. D. Broek, S. Declaye, P. Dewallef and V. Lemort, "Techno-economic survey of Organic Rankine Cycle (ORC) systems," *Renewable and Sustainable Energy Reviews*, vol. 22, p. 168–186, 1 March 2013.
- [32] S. Quoilin, V. Lemort and J. Lebrun, "Experimental study and modeling of an Organic Rankine Cycle using scroll expander," *Applied Energy*, vol. 87, p. 1260–1268, 06 August 2009.
- [33] B. Franchetti, A. Pesiridis, I. Pasmazoglou, E. Sciubba and L. Tocci, "Thermodynamic and technical criteria for the optimal selection of the working fluid in a mini-ORC," in *29th International Conference on efficiency, cost, optimization, simulation and environmental impact of energy systems*, Portoroz, 2016.
- [34] A. A. Lakew and O. Bolland, "Working fluids for low-temperature heat source," *Applied Thermal Engineering*, vol. 30, p. 1262–1268, 12 February 2010.
- [35] T. Rajabloo, "Thermodynamic study of ORC at different working and peripheral conditions," in *IV International Seminar on ORC Power Systems*, Milano, 2017.
- [36] K. Yadav and A. Sircar, "Selection of working fluid for low enthalpy heat source Organic Rankine Cycle in Dholera, Gujarat, India," *Case Studies in Thermal Engineering*, vol. 16, pp. 1-12, 22 October 2019.
- [37] M. M. Tahir and N. Yamada, "Characteristics of Small ORC System for Low Temperature Waste Heat Recovery," *Journal of Environment and Engineering*, vol. 4, no. 2, pp. 375-385, 19 March 2009.
- [38] I. E. Caceres, R. Agromayor and L. O. Nord, "Thermodynamic Optimization of an Organic Rankine Cycle for Power Generation from a Low Temperature Geothermal Heat Source," in *Proceedings of the 58th on Simulation and Modelling*, Reykjavik, 2017.
- [39] Y. Dai, J. Wang and L. Gao, "Parametric optimization and comparative study of organic Rankine cycle (ORC) for low grade waste heat recovery," *Energy Conversion and Management*, vol. 50, p. 576–582, 31 December 2008.
- [40] S. C. Kaushik, N. L. Panwar and V. S. Reddy, "Thermodynamic evaluation of heat recovery through a Canopus heat exchanger for vapor compression refrigeration (VCR) system," *Journal of Thermal Analysis and Calorimetry*, vol. 110, no. 3, pp. 1493-1499, 10 December 2011.
- [41] J. Sarkar, "Generalized pinch point design method of subcritical-supercritical organic Rankine cycle for maximum heat recovery," *Energy*, vol. 143, pp. 141-150, 15 January 2018.

- [42] C. D. Bonk, C. Laux, M. Rodder and M. Neef, "Design of a 1 kW Organic Rankine Cycle for Teaching and Research Issues," in *IV International Seminar on ORC Power Systems*, Milano, 2017.
- [43] M. A. Hafiz, "Heat transfer augmentation of porous media (metallic foam) and phase change material based heat sink with variable heat generations: An experimental evaluation," *Sustainable Energy Technologies and Assessments*, vol. 52, no. C, pp. 1-20, August 2022.
- [44] A. Shahsavari, S. Entezari, I. B. Askari and M. A. Hafiz, "The effect of using connecting holes on heat transfer and entropy generation behaviors in a micro channels heat sink cooled with biological silver/water nanofluid," *International Communications in Heat and Mass Transfer*, vol. 123, pp. 1-20, April 2021.
- [45] G. Scagnolatto, R. L. Nunes, L. C. Gómez and C. B. Tibirica, "Simulation of a Small Organic Rankine Cycle," in *17th Brazilian Congress of Thermal Sciences and Engineering*, Brazil, 2018.
- [46] A. Saha, "Energy and Exergy Analysis of Waste Heat Recovery Systems using Organic Rankine Cycle," Dhaka, 2016.
- [47] R. Kong, T. Deethayat, A. Asanakham, N. Vorayos and T. Kiatsiriroat, "Thermodynamic performance analysis of a R245fa organic Rankine cycle (ORC) with different kinds of heat sources at evaporator," *Case Studies in Thermal Engineering*, vol. 13, pp. 1-10, 29 December 2018.
- [48] E. Özdemir and M. Kilic, "Thermodynamic Analysis of Basic and Regenerative Organic Rankine Cycles Using Dry Fluids from Waste Heat Recovery," *Journal of Thermal Engineering*, vol. 4, no. 5, pp. 2381-2393, July 2018.
- [49] A. H. Bademlioglu, R. Yamankaradeniz and O. Kaynakli, "Exergy Analysis of the Organic Rankine Cycle Based on the Pinch Point Temperature Difference," *Journal of Thermal Engineering*, vol. 5, no. 3, pp. 157-165, April 2019.
- [50] S. Shet, O. Patil and N. Agrawal, "Energetic and exergetic studies of modified CO<sub>2</sub> transcritical refrigeration cycles," in *12th IIR Gustav Lorentzen Conference on Natural Refrigerants*, Edimbourg, 2016.
- [51] H. Chen, D. Y. Goswami, M. M. Rahman and E. K. Stefanakos, "Energetic and exergetic analysis of CO<sub>2</sub>- and R32-based transcritical Rankine cycles for low-grade heat conversion," *Applied Energy*, vol. 88, pp. 2802-2808, 19 February 2011.
- [52] O. A. Oyewunmi, S. Lecompte, M. D. Paepe and C. N. Markides, "Thermoeconomic analysis of recuperative sub - and transcritical organic rankine cycle systems," in *IV International Seminar on ORC Power Systems*, Milano, 2017.
- [53] E. Cayer, N. Galanis, M. Desilets, H. Nesreddine and P. Roy, "Analysis of a carbon dioxide transcritical power cycle using a low temperature source," *Applied Energy*, vol. 86, no. 7-8, pp. 1055-1063, July-August 2009.
- [54] K. S. Rawat, H. Khulve and A. K. Pratihari, "Thermodynamic Analysis of Combined ORC-VCR System Using Low Grade Thermal Energy," *International Journal for Research in Applied Science & Engineering Technology*, vol. 3, no. 7, pp. 515-522, July 2015.
- [55] S. Aphornratana and T. Sriveerakul, "Analysis of a combined Rankine–vapour–compression refrigeration cycle," *Energy Conversion and Management*, vol. 51, no. 12, pp. 2557-2564, 9 June 2010.
- [56] B. Saleh, "Energy and exergy analysis of an integrated organic Rankine cycle-vapor compression refrigeration system," *Applied Thermal Engineering*, vol. 141, pp. 697-710, 14 June 2018.
- [57] P. D. Malwe, B. Gawali, M. Choudhari, R. Dhalait and N. Deshmukh, "Energy and Exergy Analysis of an Organic Rankine Cycle Integrated with Vapor Compression Refrigeration System," *Advances and Applications in Mathematical Sciences*, vol. 20, no. 10, pp. 2137-2150, August 2021.
- [58] F. Moles, J. Navarro-Esbrí, B. Peris, A. M. Babiloni and K. Kontomaris, "Thermodynamic analysis of a combined organic Rankine cycle and vapor compression cycle system activated with low temperature heat sources using low GWP fluids," *Applied Thermal Engineering*, vol. 87, pp. 444-453, 27 2015 May.
- [59] H. Wang, R. Peterson, K. Harada, E. Miller, R. Ingram-Goble, L. Fisher, J. Yih and C. Ward, "Performance of a combined organic Rankine cycle and vapor compression cycle for heat activated cooling," *Energy*, vol. 36, no. 1, pp. 447-458, 11 November 2010.
- [60] W. Sun, X. Yue and Y. Wang, "Exergy efficiency analysis of ORC (Organic Rankine Cycle) and ORC-based combined cycles driven by low-temperature waste heat," *Energy Conversion and Management*, vol. 135, pp. 63-73, 1 March 2017.
- [61] K. H. Kim and H. Perez-Blanco, "Performance analysis of a combined organic Rankine cycle and vapor compression cycle for power and refrigeration cogeneration," *Applied Thermal Engineering*, vol. 91, pp. 964-974, 21 August 2015.
- [62] M. Asim, M. K. Leung, Z. Shan, Y. Li, D. Y. Leung and M. Ni, "Thermodynamic and Thermo-economic Analysis of Integrated Organic Rankine Cycle for Waste Heat Recovery from Vapor Compression Refrigeration System," in *World*

*Engineers Summit – Applied Energy Symposium & Forum: Low Carbon Cities & Urban Energy Joint Conference*, Singapore, 2017.

- [63] M. Imran, M. Usman, B.-S. Park and Y. Yang, "Comparative assessment of Organic Rankine Cycle integration for low temperature geothermal heat source applications," *Energy*, vol. 102, pp. 473-490, 1 May 2016.
- [64] M. Asim, F. Kashif, J. Umer, J. Z. Alvi, M. Imran, S. Khan, A. W. Zia and M. K. H. Leung, "Performance Assessment and Working Fluid Selection for Novel Integrated Vapor Compression Cycle and Organic Rankine Cycle for Ultra Low Grade Waste Heat Recovery," *Sustainability*, vol. 13, no. 21, pp. 1-16, 20 October 2021.
- [65] I. H. Bell, J. Wronski, S. Quoilin and V. Lemort, "Pure and Pseudo-pure Fluid Thermophysical Property Evaluation and the Open-Source Thermophysical Property Library CoolProp," *Industrial & Engineering Chemistry Research*, vol. 53, no. 6, pp. 2498-2508, 13 January 2014.

443  
444